SEISMIC WAVES AND EARTHQUAKE LOCATION

J.R. Kayal

Geological Survey of India, 27, J.L. Nehru Road Road, Kolkata – 700 016
email : jr_kayal@hotmail.com

SEISMIC WAVES

Two basic types of elastic waves or seismic waves are generated by an earthquake; these are *body waves* and *surface waves*. These waves cause shaking that is felt, and cause damage in various ways. These waves are similar in many important ways to the familiar waves in air generated by a hand-clap or in water generated by a stone thrown into water.

Body Waves

The body waves propagate within a body of rock. The faster of these body waves is called *Primary wave* (*P-wave)*, or *longitudinal wave or compressional wave,* and the slower one is called *Secondary wave* (*S-wave)* or *shear wave.*

P-wave

The P-wave motion, same as that of sound wave in air, alternately pushes (compresses) and pulls (dilates) the rock (Fig. 1). The motion of the particles is always in the direction of propagation. The P-wave, just like sound wave, travels through both solid rock such as granite and liquid material such as volcanic magma or water. It may be mentioned that, because of sound like nature, when P-wave emerges from deep in the Earth to the surface, a fraction of it is transmitted into atmosphere as sound waves. Such sounds, if frequency is greater than 15 cycles per second, are audible to animals or human beings. These are known as *earthquake sound*.

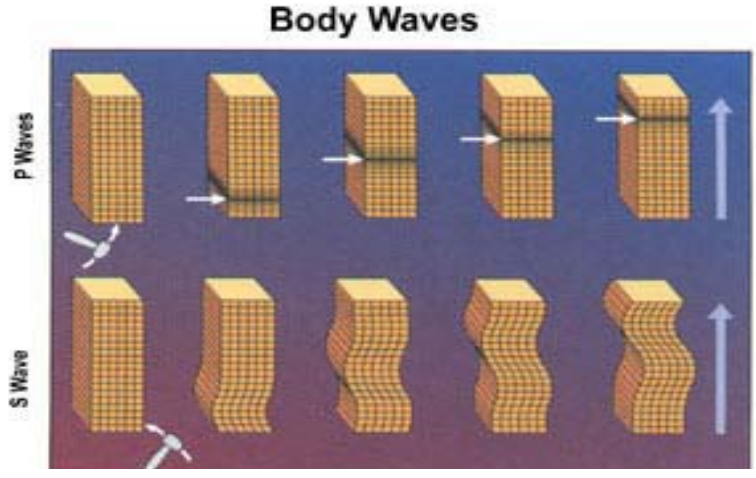

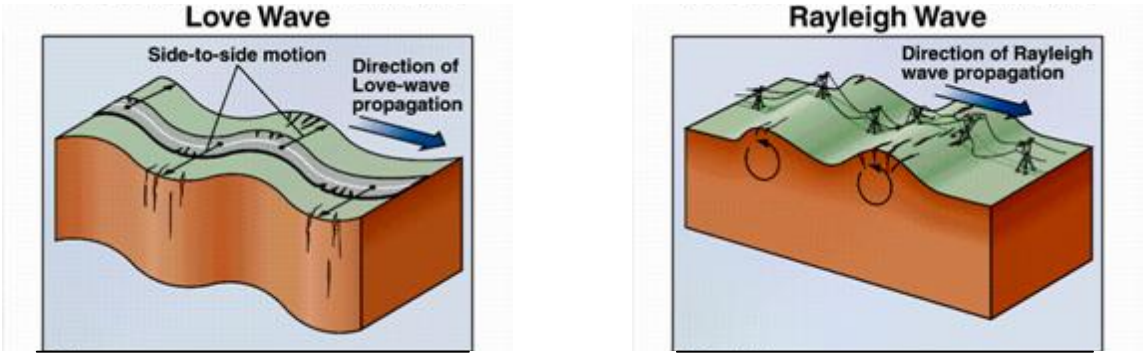

Fig 1 : Seismic wave propagation

The relation between compressional or P-wave velocity (V_p) and the elastic constants E (Young's modulus), σ (Poisson's ratio), K (bulk modulus), μ (rigidity modulus), λ (Lame's constant) and density ρ is given as follows:

$$V_p = \left\{ \frac{(\lambda + 2\mu)}{\rho} \right\}^{\frac{1}{2}} \qquad (1)$$

S-wave

It is known that the S-wave or the *shear wave* shears the rock sideways at right angle to the direction of propagation (Fig. 1). As shear deformation cannot be sustained in liquid, shear waves cannot propagate through liquid materials at all. The outer portion of Earth's core is assumed to be liquid because it does not transmit shear waves from earthquakes. The particle motion of the S-wave is perpendicular (transverse) to the propagation. If the particle motion of the S-wave is up and down in vertical plane; it is named S_V wave. However, S-wave may also oscillate in horizontal plane, which is called S_H wave.

The relation between S-wave velocity V_S, the elastic constants and density is given as:

$$Vs = \left(\frac{\mu}{\rho} \right)^{\frac{1}{2}} \qquad (2)$$

The velocity ratio

V_P/V_S

Comparing the equations (1) and (2), we find that the ratio of compressional to shear wave velocity is

$$\frac{Vp}{Vs} = \left(\frac{K}{\mu} + \frac{4}{3}\right)^{\frac{1}{2}} = \left(\frac{1-\sigma}{\frac{1}{2}-\sigma}\right)^{\frac{1}{2}} \qquad (3)$$

For most consolidated rock $V_P/V_S \simeq \sqrt{3}$. In this context, it may be mentioned that amplitudes of S-waves are generally five times larger than those of P-waves. This follows from the far field term of Green's function when modeling earthquake shear sources taking into account $V_p \simeq \sqrt{3}\, V_s$. Also, the periods of S-waves are longer, at least by a factor of $\sqrt{3}$, than those of P-waves due to differences in wave propagation velocity.

Surface Waves

The second general type of earthquake wave is called *surface wave*, because its motion is restricted to near the ground surface. Such waves correspond to ripples of water that travel across a lake. The wave motion is located at the outside surface itself, and as the depth below this surface increases, wave displacement becomes less and less. Surface waves in earthquakes can be divided into two types; *Love waves* and *Rayliegh waves.* The Love waves are denoted as LQ (or G) and the *Rayleigh* waves as LR (or R). While Rayleigh waves exist at any free surface, Love waves require some kind of wave guide formed by velocity gradient. Both conditions are fulfilled in the real Earth.

Love Wave (LQ)

The British mathematician A.E.H. Love demonstrated that if an S_H ray strike a reflecting horizon near surface at post critical angle, all the energy is 'trapped' within the wave guide (Love, 1911). These waves propagate by multiple reflections between the top and bottom surface of the low speed layer near the surface. The waves are called *Love waves,* and denoted as LQ or G. Its motion is same as that of the S-waves that have no vertical displacement. It moves the ground from side to side in a horizontal plane parallel to Earth's surface, but at right angle to the direction of propagation (Fig. 1); so the wave motion is horizontal and transverse.

The Love wave velocity (V_L) is equal to that of shear waves in the upper layer (V_{S1}) for very short wave lengths, and to the velocity of shear waves in the lower layer (V_{S2}) for very long wave lengths, i.e.

$$\text{Velocity } V_{S1} < V_L < V_{S2} \qquad (4)$$

The effects of Love waves are result of the horizontal shaking, which produces damage to the foundation of structures. Love waves do not propagate

through water, it affect surface water only. It causes the sides of the lakes and ocean bays move backwards and forwards, pushing the water sideways like the sides of a vibrating tank.

Rayleigh Wave (LR)

Rayleigh (1885) demonstrated that the surface boundary condition can be satisfied leading the existence of a 'coupled' and 'trapped' P-S_V wave travelling along the surface, such as the Earth-air interface, with a velocity lower than shear velocity, and with an amplitude decaying exponentially away from the surface. This second type of surface wave is known as *Rayleigh wave*. In general the surface waves with periods 3 to 60s are denoted R or LR. Like rolling ocean waves, the *Rayleigh waves* develop the particle motion both vertically and horizontally in a vertical plane pointed in the direction of wave propagation. Since Rayleigh waves generate from coupled P and S_V waves the particle motion is always in vertical plane, and due to phase shift between P and S_V the particle motion is elliptical and retrograde (counter clockwise) with respect to the direction of propagation (Fig.1). The amplitude of the motion decreases exponentially with depth below the surface.

The speed of *Rayleigh wave* (V_R) is about 9/10th of shear wave (V_S) in the same medium; the relation is given as

$$V_R < 0.92\ V_S \qquad (5)$$

For short wave-lengths V_{Rg} corresponds to 9/10 V_S of the material comprising the surface layer. For very long wave-lengths, the V_{RL} corresponds to 9/10 V_S of the substratum material since effect of the surface layer is negligible when most of the waves travel in the zone below it. As seen from the above equations, S-wave is slower than P-wave, and *Rayleigh wave* is slower than Love wave. Thus as the waves radiate outwards from an earthquake source, the different types of waves separate out from one another in a predictable pattern (Fig. 2).

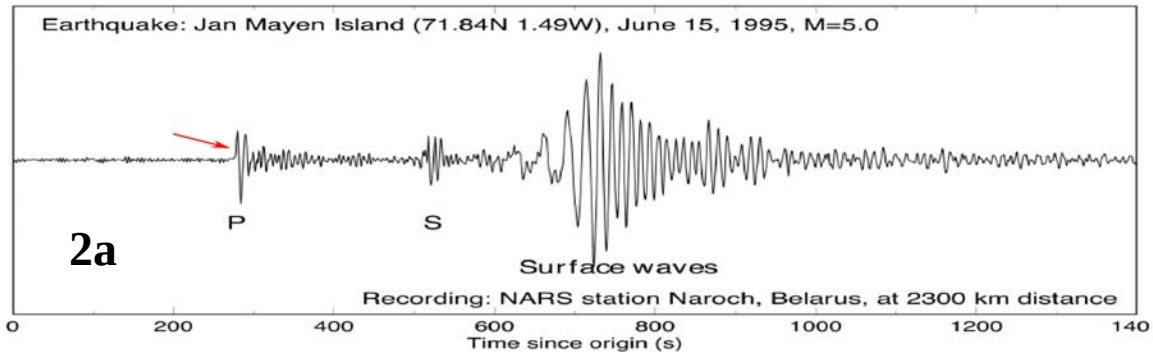

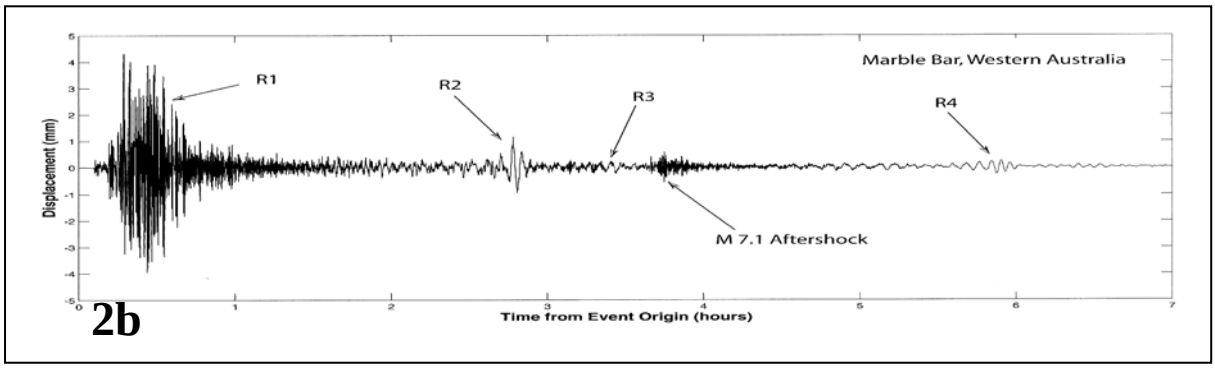

Fig 2a: Seismogram showing body waves and surface waves
Fig 2b: Seismogram of the 2004 Sumatra earthquake showing different seismic phases

Guided Waves

Channel Waves

Guided waves exist in a layered medium such that its properties change only vertically and not horizontally. It is most significant when there is a channel or layer between two discontinuities. For example, coal seam which is a low velocity layer, if sandwiched between two high velocity layers, say sandstones, can act as a channel through which body waves will travel as guided waves or channel waves which may also include surface waves (Evison, 1955). There is a great deal of literature on channel wave seismology for coal exploration (e.g. Krey, 1963; Dresen and Freystatter, 1976).

L_g Waves

L_g waves are one kind of guided waves in the continental crust. These are essentially high frequency Love waves at regional distances of thick continental crust. It travels over long continental paths with relatively little loss of energy, but is cut off abruptly when the path has even a small oceanic segment. The subscript L_g refers to granitic layer. L_g waves being critically incident on the *Mohorovičić'* (Moho) discontinuity propagate by multiple reflections within the crust with a typical velocity 3.5 km/s. These waves dominate the seismograms, specially the horizontal channels. L_g is usually recorded at epicentral distances of about 5^0 and larger. Ewing et al. (1957) identified it and defined it as a tool for finding boundary of continental structure.

R_g wave

At local or regional distances high frequency fundamental mode of *Rayleigh waves* are labeled as R_g. The presence of short period R_g in the seismogram is a reliable indicator of very shallow event (like earthquake, nuclear explosion, mine burst etc.). In other words, absence of R_g *indicates* deeper natural event. The short period R_g waves travel as guided waves through continental crust with velocity 3 km/s; their range of propagation is limited to 600 km or less.

T-waves

The term T-wave in seismology literally means *Tertiary wave* or third wave. These are slow waves, which arrive long after the faster Primary (P) wave or Secondary (S) wave. These waves are observed at costal seismic stations that record sub-ocean earthquakes at regional distances.

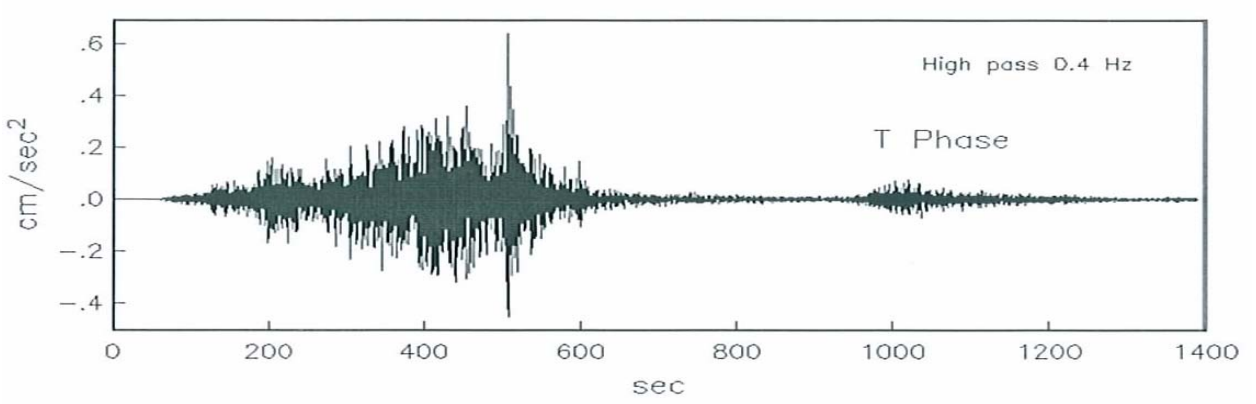

Similar to low velocity layer in the upper mantle, there is also low velocity channel in deep ocean. Depending on the salinity and temperature of sea water, the sound velocity decreases to a minimum of about 1.5 km/s from sea surface to 700-1300 m depth, and again increases below this depth. This depth region of low velocity in ocean is called SOFAR (Sound Fixing and Ranging channel). Propagation of T-waves generally by SOFAR channel (Bullen and Bolt, 1985) or by multiple reflections between the sea floor and sea surface (Bath and Sahidi, 1974) is every efficient at distances as large as 80^0. They show a small gradual beginning, and a gradual amplitude increase, arriving after P and S. The duration can be explained by dispersion. They exhibit rather monochromatic oscillations (Fig. 3). These waves are recorded by SOFAR *hydrophones, ocean bottom seismometers* (OBS) or seismographs which are located near to the coast. Unlike P-waves, there is no sharp onset for T-wave group. The appearance of T-phases on seismograms depends largely on the ocean bottom topography, water and land conversion and transmission properties. Ewing et al. (1952) demonstrated that T phase propagates as sound

waves through the water and as body waves over the land path, i.e., from the coast or from the continental shelf to the seismic station.

SEISMIC WAVES AND GROUND SHAKING

The body waves (P and S-waves), when move through the layers of rock in the crust, they are reflected and or refracted at the interfaces between the rock types or layers. When P and S waves reach the surface of the ground, most of their energy is reflected back into the crust. Thus, the surface is affected simultaneously by upward and downward moving waves. After a few shakes, a combination of two kind of waves is felt in ground shaking. A considerable amplification of shaking occurs near the surface. This surface amplification enhances the shaking at the surface of the Earth. On the other hand, earthquake shaking below ground surface, say in the mine, is much less. Again combination of two kinds of waves in shaking is not felt at sea. The only motion felt on ship is from the P-waves, because S-waves cannot travel through water beneath the ship. A similar effect occurs as sand layers liquify in earthquake shaking, which is appropriately known as *liquefaction*. There is progressive decrease in the amount of S-wave energy that is able to propagate through liquefied layers; ultimately only P-wave can pass through it.

The above description is not adequate to explain the heavy shaking due to a large earthquake. The effect of surface waves (Love wave and Rayleigh wave), and various kinds of mixed seismic waves including converted and reflected seismic phases at the rock interfaces complicate the matter, and type of ground shaking is further muddled together. The horizontal and transverse motion of the Love waves, and elliptical and retrograde motion of the Rayleigh waves cause severe damage to the foundations of engineering structures and buildings.

The ground shaking is also much affected by soil conditions and topography. For example, in weathered surface rocks, in alluvium and water filled soil, the amplification of seismic waves may increase or decrease as the waves reach to the surface from the more rigid basement rocks. Also at the top or bottom of a ridge, shaking may intensify, depending on the direction from which waves are coming and whether the wave lengths are short or long. The site amplifications play an important role in *microzonation* study (e.g. Field and Jacob, 1995).

SEISMIC PHASES AT THE ROCK BOUNDARIES

The body waves (the P and S waves) are reflected or refracted at the interfaces between rock types. In addition to reflection or refraction of one type, the seismic waves are also converted to other types. As illustrated in Fig. 4, P-wave travels upwards and strikes the bottom of a layer of different rock type; part of its energy will pass through the upper layer as P-wave and part as converted S-wave, which is known as P to S conversion (or P_S phase), and part of energy will be reflected back downwards as P and S waves. Similar reflection, refraction and conversion may occur with S-wave. All these *converted phases* are useful for velocity and geological structure study.

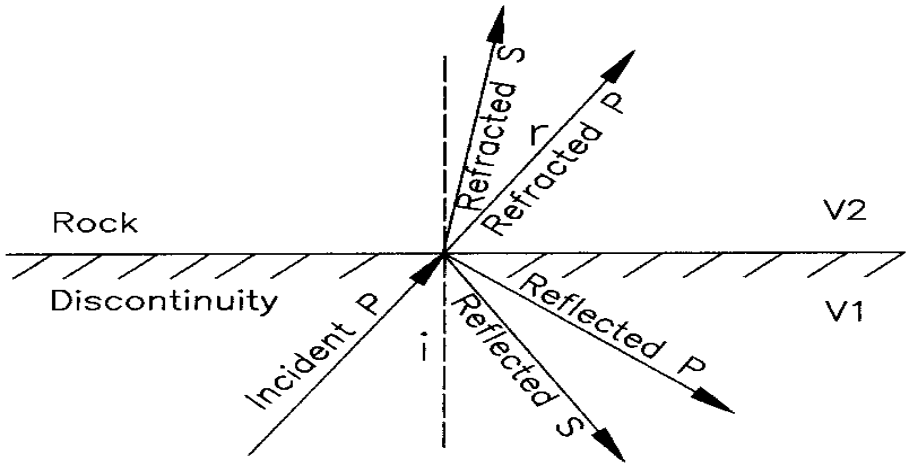

Fig4 a: Phase conversion at the rock boundary

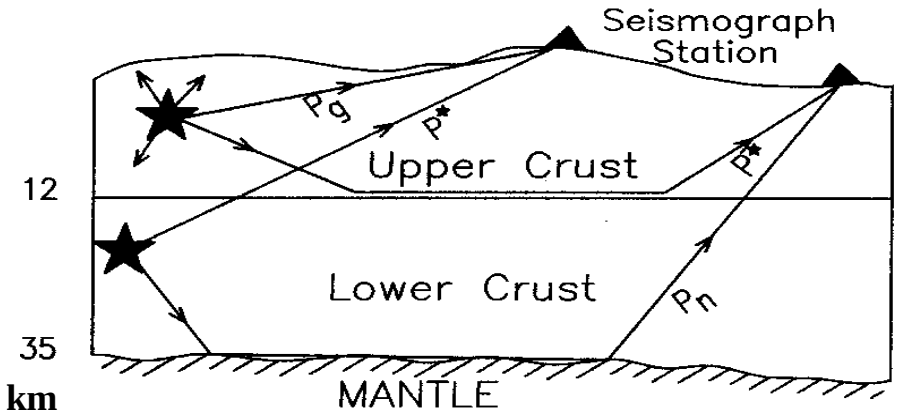

Fig 4 b: Direct and Refracted P-phases

Snell's law

The Fig. 4 demonstrates the law of reflection, i.e. angle of incidence i is equal to angle of reflection r_1. The lower part of the diagram demonstrates the law of refraction, or Snell's law. It is easily deduced that

$$\frac{Sin\,i}{Sin\,r_2} = \frac{V_1}{V_2} \qquad (6)$$

where r_2 is the angle of refraction, V_1 and V_2 are the velocity of the upper and lower layer respectively. This formula can be extended to the case of reflection or refraction of a wave of different type, e.g. reflected or refracted S from an incident P, leading to a generalised form of Snell's law:

$$\frac{V}{Sin\,i} = \text{constant } (\rho) \qquad (7)$$

where V stands for either V_P or V_S on either side of the boundary, and *i* is the angle between the corresponding ray (incident, reflected or refracted) and the normal on the same side, and *p* is called *seismic parameter or ray parameter*.

The ray parameter is constant for the entire travel path of a ray. The consequence of a ray traversing material of changing velocity, V, is a change in incidence angle, i, with respect to a reference plane. As the ray enters material of increasing velocity, the ray is deflected toward the horizontal. Conversely, as it enters material of decreasing velocity, it is deflected towards the vertical. If the ray is traversing vertically, then *p=o*, and the ray will have no deflection as velocity changes.

SEISMIC PHASES AT SHORT DISTANCES

P and S arrivals

The seismic phases generated by an earthquake at a shallow depth (d < 10 km) and recorded by a station within a few km of the epicentre, are generally identified as direct P and S arrivals. A seismogram is illustrated in Fig. 5. The apparent velocities of P and S, as determined from time – distance curves, are about 5.5 and 3.2 km/s respectively in the shallow crust.

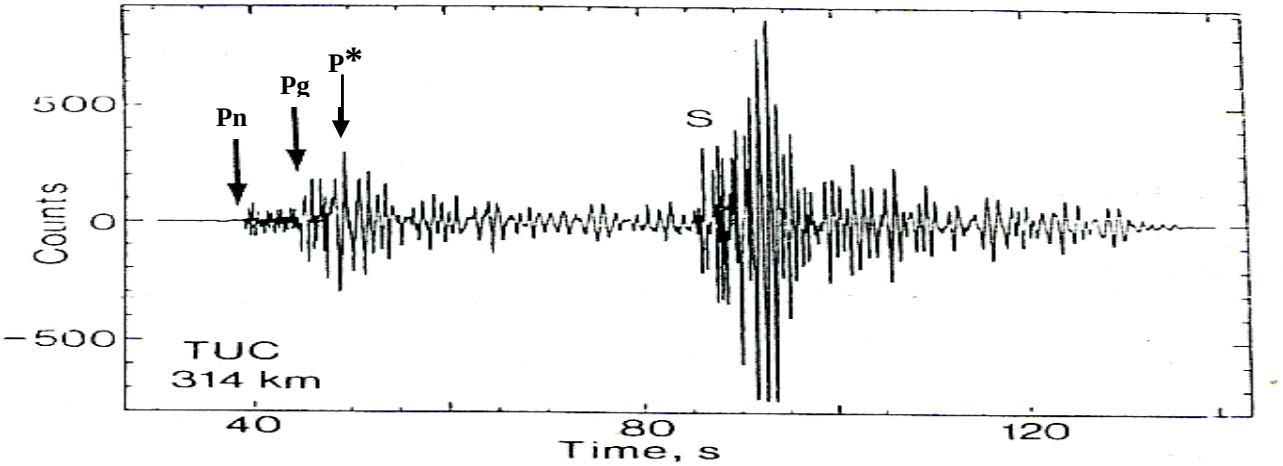

Fig 5: Seismogram showing different seismic phases for a local earthquake.

P_n and S_n arrivals

In 1909, A. Mohorovičić identified refracted P_n and S_n arrivals from the interface between the crust and mantle, the layers of lower and higher velocity. He made this discovery on seismograms of an earthquake with epicentre not far from his seismograph station. He found that there is a *critical distance*, generally in the range 100-150 km, beyond which P and S waves are refracted, and arrive with small and long period motion. He designated these phases as P_n and S_n respectively. These are also called *head waves.* The head wave travels with faster apparent velocity along the refractor, and it becomes the *first* arrival. The incidence angle at which the ray is refracted at 90^0 along the refractor is called the *critical angle.* The ray-geometry is illustrated in Fig. 4. If $V_2 > V_1$, three primary travel paths exist between the source and the receiver : (i) direct arrival which travels in a straight line connecting the source and receiver, (ii) reflected arrival and (iii) a head wave. Additional rays involving multiple reflections will also exist, and make the seismogram complicated. The head waves are followed by the larger and sharper impulse of short period direct P and S arrivals. An example of P_n, Pg, P* and S phases is illustrated in Fig. 5. The apparent velocities of P_n and S_n as read from their time-distance curves are about 8.0 and 4.6 km/s respectively, which are the upper mantle velocities. The surface of separation between the crust and upper mantle is termed as *Moho discontinuity.*

P_g, S_g and P^*, S^* arrivals

Later study of seismograms by many investigators revealed further complexity. Conrad observed a small sharp impulse between P_n and P which he named P^*, and attributed it to refraction through an intermediate layer with a velocity of about 6.5 km/s. The upper boundary of this layer had been called *Conrad discontinuity.* Seismologists have, more or less, accepted the Conrad discontinuity as separating predominantly *granitic layer* above it and *basaltic layer* below, within the crust, and proposed notations as P_g, S_g and P^*, S^*. The P_g and S_g are practically the same as P and S.

Converted Phases

Although conversions of seismic phases at the Conrad discontinuity and at the Moho discontinuity are well illustrated, there is still controversy about the Conrad discontinuity. The conversion of seismic phases P to S (P_S) or S to P (S_P) at the *Moho* discontinuity is well established (Fig. 4), (e.g. Cook et al., 1962; Kayal, 1986). The reflected rays from the Moho discontinuity are labeled as P_P (or PmP) and S_S or (SmS).

In rare instances, additional phases between P_n, P_g are present on the seismograms. The P and S leave the focus, travel upward and get reflected as P and S at the free surface and continue further as P_n, S_n. Notations for these phases are given as ${}_pP_n$ and ${}_sS_n$ respectively. For a more detailed description of seismic phases of local, regional and teleseismic events readers are referred to Anatomy of Seismogram by Kulhanek, (1990). A detailed nomenclature of seismic phases for local, regional and teleseismic events is given in Table 1.

Table 1

Nomenclature of Seismic Phases (after Kuthanek, 2002)

Symbol	Meaning
Local and regional events	
P, S	Direct compressional or shear wave traveling through the upper crust (observed only at very short epicentral distances)
Pg, Sg	Compressional or shear wave in the granitic layer of the crust
PmP, SmS	Compressional or shear wave reflected at Moho
Pn, Sn	Compressional or shear wave traveling along (just beneath) the Moho discontinuity, so called head wave
P, S* (or Pb, Sb)*	Compressional or shear wave traveling along (just beneath) the Conrad discontinuity
PPn	Depth phase that leaves the focus upward as *P*, is reflected as *P* at the free surface and continues further as *Pn*
SPn	Depth phase that leaves the focus upward as *S*, is reflected and converted into *P* at the free surface and continues further as *On*
Rg	Short-period crustal surface wave of Rayleigh type
Lg	Guided crustal wave traversing large distances along continental paths
T	Compressional wave propagating through the ocean (Tertiary wave). *T* phases are occasionally observed even at larger teleseismic distances
TPg(TSg,TRg)	Wave that travels the ocean and land portion of the total transmission path as *T* and *Pg (Pg,Rg)*, respectively.

Teleseismic events

P,S	Direct compressional or shear wave, so called elementary or main wave
PP,PPP,SS,SSS	*P* or *S* wave reflected once or twice at the Earth's surface
SP	*S* wave converted into *P* upon reflection at the Earth's surface
PPS,PSP,PSS	*P* wave twice reflected/converted at the Earth's surface.
PcP ,ScS	*P* or *S* wave reflected at the core-mantle boundary
PcS, Scp	*P* or *S* wave converted respectively into *S* or *P* upon reflection at the core-mantle boundary.
pP,pS,pPP,pPS, etc.	Depth phase that leaves the focus upward as *P*(*p* leg), is reflected/converted at the free surface and continues further as *P,S,PP,PS,* etc.
SP,sS,sPP,sPS, etc.	Depth phase that leaves the focus upward as *S*(*s* leg), is reflected/converted at the free surface and continues further as *P,S,PP,PS,* etc.
pMP	*P* wave reflected at the underside of Moho
pwP	*P* wave reflected at the water surface
PdP	*P* wave reflected at the underside of a discontinuity at depth *d* in the upper part of the Earth. *d* is given in kilometers, e.g., *P*400*P*
Pc,Sc or Pdif, Sdif	*P* or *S* wave that is diffracted around the core-mantle boundary
PKP (or P')	*P* wave traversing the outer core
PKS	*S* wave converted into *S* on refraction when leaving the core
SKS	*P* wave traversing the outer core as *P* and converted back into *S* when again entering the mantle
SKP	*S* wave converted into *P* on refraction into the outer core.
PKP1,PKP2 or PKP_{BC}, PKP_{AB}	Different branches of *PKP*
PKiKP	*P* wave reflected at the boundary of the inner core
PKIIKP	*P* wave reflected from the inside of the inner-core boundary
PKKP	*P* wave reflected from the inside of the core-mantle boundary
PmKP(m=3,4,…)	*P* wave reflected *m* – 1 times from the inside of the core-mantle boundary.
SmKS(m=3,4,…)	*S* wave converted into *P* on refraction at the outer core, reflected *m* – 1 times from the inside of the core-mantle boundary and finally converted back into *S* when again entering the mantle
PKPPKP (or P'P')	*PKP* wave reflected from the free surface, passing twice through the core
P'dP'	*PKP* reflected at the underside of the discontinuity at depth *d* in the upper part of the Earth, *d* is given in kilometers
LR	Surface wave of Rayleigh type
LQ	Surface wave of Love type
G	Mantle wave of Love type
R	Mantle wave of Rayleigh type
G1, G2	*LQ*-type mantle wave that travels the direct and anticentre routes. Waves that have, in addition, traveled once or several times around the Earth are denoted *G3,G4,G5, G6, etc.*
R1, R2	*LR*-type mantle wave that travels the direct and anticenter routes.

Waves that have, in addition, traveled once or several times around the Earth are denoted *R3,R4,R5, R6, etc.*

Teleseismic Waves and Interior of the Earth

Virtually all our direct informations about the interior of the Earth are derived from the observations of earthquake generated seismic waves only. Since much of the Earth is an elastic solid, two kinds of body waves can propagate through the Earth. The path of the waves are affected by two main discontinuities in the Earth; one at a depth 30-60 km, and the other at a depth of 2900 km. The first one is called the *Moho discontinuity* which is of special importance in interpreting seismograms at short epicentral distances upto a few hundred kilometres as discussed above. Evidence of the second discontinuity was discovered by Wiechert and by Oldham in 1906, but correct identification and determination of depth of this discontinuity was made by Gutenberg (1914), hence called *Gutenberg discontinuity*. These two discontinuities divide the Earth internally into an outer shell, called the *crust*, an intermediate shell, called the *mantle* and a central *core*. The major divisions of the Earth's interior are shown in (Fig.6). The mantle is subdivided into upper mantle and lower mantle, and core is subdivided into outer core and inner core.

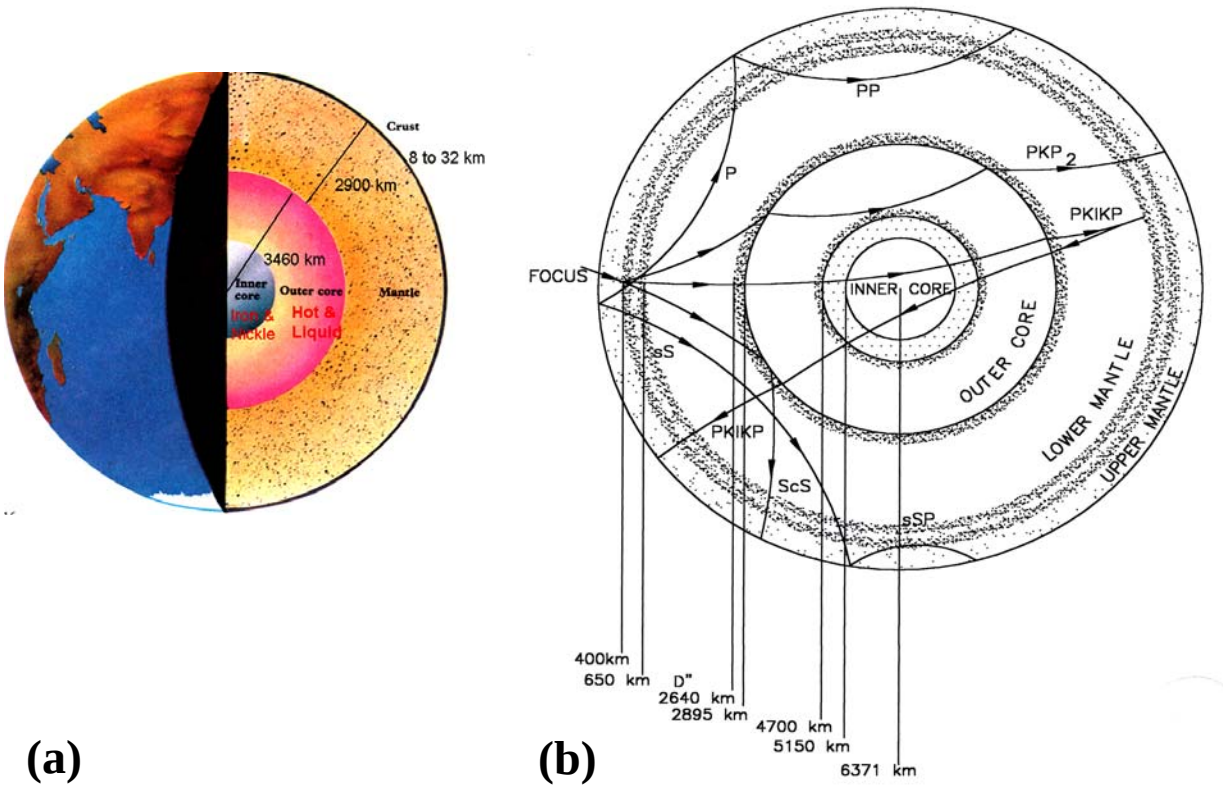

Fig 6: (a) Major discontinuities of the Earth and (b) the seismic waves.

Seismic waves arriving at a distance beyond 10^0 upto about 30^0 mainly travel through the upper mantle (Moho to 410 km) and through the transition zone to the lower mantle (410-660 km). The strong discontinuities in the transition zone have strong *seismic impedance* (i.e. the quantity Vxρ, that increases with the increase of velocity V and density ρ). This results triplications of the travel-time curve for P waves and S waves that gives rise to complicated short-period wave forms consisting of sequence of successive onsets with different amplitudes. The base of the transition zone is labeled as D″ region (Bullen, 1949), which may be caused by either chemical differentiation in the mantle or by chemical reactions between core and mantle (e.g. Lay, 1989; Jeanloz, 1993).

At epicentral distances between about 30^0 and 100^0, the P and S waves travel through the lower mantle that is characterized by a rather smooth positive velocity and density gradient. The seismograms are clearly structured with P and S arrivals, followed by multiple surface and core-mantle boundary (CMB) reflections on conversions (Fig 7). The existence of the great velocity reductions across the CMB causes seismic wave energy to diffract into the geometric shadow zone at distances greater than 100^0.

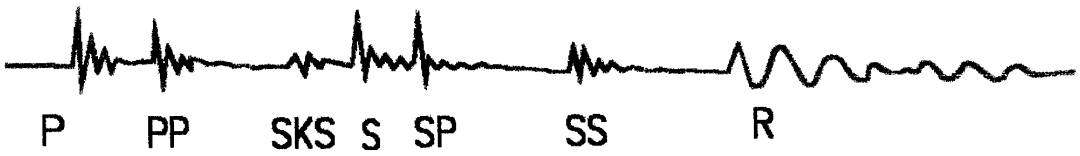

Fig.7 : Seismogram showing converted seismic phases from CMB.

Beyond 100^0, only P-wave enters outer core, and reach surface. There is a dramatic reduction of P-wave velocity, from 13.7 km/s in the lower most mantle to 8.0 km/s in the upper outer core. This P-wave form a core shadow. Oldham (1906) first observed that a P-wave arriving at the antipodes of an earthquake was late, in comparison with the expected arrival time. He proposed the existence of core of lower velocity than outer region, and predicted the presence of a *shadow zone*. Gutenberg (1912) verified that there was a shadow zone for P between $\Delta = 105^o$ and $\Delta = 143^o$ with strong arrivals just beyond 143^o. Gutenberg estimated the depth to the core boundary as 2900 km which stood unchallenged until very recently. The shadow zone of the core is not complete, there being arrivals of P-waves of small amplitude through the entire zone. Lehmann (1935) suggested that these arise from *inner core* of higher velocity within the main core. Her proposal of inner core became widely accepted.

The teleseismic arrivals, corresponding to different paths, are illustrated in Fig. 7. The letters P and S are used to designate reflected or refracted waves outside the core. The subscripts **c** and **i** denote reflections from the outer and inner core boundaries respectively, while the letters **K** and **I** indicate P waves through outer and inner core. A wave of S type through the outer core has not been observed. We have also phases such as PP, reflected from the Earth's surface. The Table 1 gives details of different local, regional and teleseismic phases. For global earthquakes and global seismology, readers may refer to the excellent book by Lay and Wallace (1995).

Global Travel-time Models

The velocities of P and S waves provide information about the Earth's interior. When an earthquake occurs, waves from it are recorded at known locations and at known times, although the latter is not free of error. The travel-time curves are always plotted against the arc distance (Δ). The time interval S-P measured at any station gives a unique indication of arc distance to the earthquake, and distances determined from three or more stations locate the source uniquely. The weakness in this method is, however, a time-distance curve must be established before the source can be located, but this location is essential for construction of the curve. So, in the early history of seismology time-distance curve was constructed for the earthquakes which were precisely located by direct observations or by very close seismographs (Wiechert and Zoppritz, 1907).

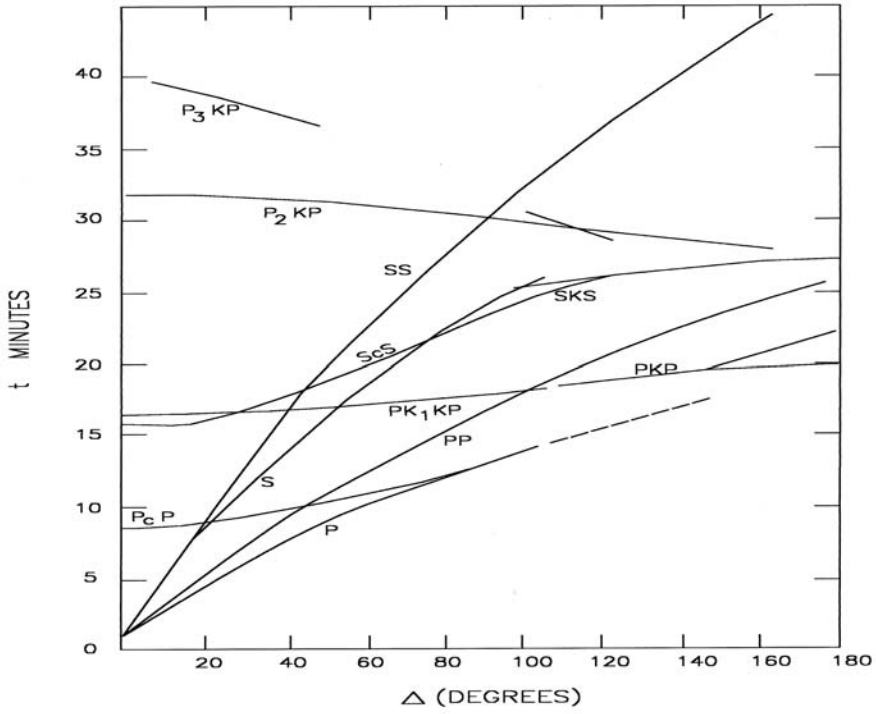

Fig 8: Global travel time curves

Revision of time-distance curves was accomplished by Jeffreys (1932) by least-square technique. In this method, the residuals i.e. the differences between the observed arrival times of P or S and their computed arrival times based on preliminary location and preliminary travel-time curves, are minimized by simultaneous adjustment of epicentre coordinates, origin time and travel-time curve. Number of equations become very great as more earthquakes and stations are utilised. However, Jeffreys devised a method of treating the observations in groups. This analysis in collaboration with Bullen produced the Jeffreys-Bullen (J-B) Tables (1935, 1940). This gives adjusted travel times for P and S waves and also for reflected and refracted waves as functions of the arc distances Δ (Fig. 8). Bullen (1965) has described the production of these tables, including the derivation of the correction for the elliptical shape of the Earth. This has provided basic information of body wave seismology, which in turn yielded Earth models that are still taken as standards for reference. Improvement in observational technique, specially timing and availability of large artificial explosions, have permitted correction to the J-B tables; and the new tables for P-waves were published by Herrin (1968).

In 1987 the International Association of Seismology and Physics of the Earth's Interior (IASPEI) initiated a major international effort to construct new global travel-time tables for earthquake location and phase identification. As a result of this, two models were developed : IASP 91 and SP6 (Kennett and Engdahl, 1991). The most significant differences between these new models and the older J-B travel-time model are in the upper mantle and core. The IASP 91 model has been adopted as the global reference model for International Data Centre in Vienna.

Subsequently Kennett et al. (1995) began with the best characteristics of the IASP 91 and SP 6 models, and further improved the global reference model to AK 135. The AK 135 model differs from IASP 91 only in velocity gradient for the D" layer and in the baseline for S-wave travel times. The model AK 135, the body wave travel-time tables and plots, are available via http : // rses.anu.edu.au/seismology/ak135/intro.html, and can be downloaded and printed in postscript.

Wave Attenuation

Seismic attenuation is caused by either intrinsic anelasticity or scattering effects. The intrinsic anelasticity is associated with small scale crystal dislocations, friction and movement of interstitial fluids. This effect is called *intrinsic attenuation*. The scattering effect is, on the other hand, is an elastic process of redistributing wave energy by reflection, refraction and conversion

that occur at discontinuities in the medium. This scattering of energy at small scale heterogeneities along travel paths reduce amplitudes of the seismic waves. These effects are called *scattering attenuation*.

The wave attenuation is usually expressed in terms of dimensionless *quality factor* Q, where

$$Q = 2\pi E/\Delta E \qquad (8)$$

The ΔE is the dissipated energy per cycle. Large energy loss means low Q and vice versa, i.e. Q is inversely proportional to the attenuation.

We can also write an equation for amplitude as a function of distance traveled (Aki and Richard, 1980) :

$$A(\chi) = Aoe^{-(f\pi/Q)\chi} \qquad (9)$$

It is obvious from eq. ….. that for a constant value of Q a high frequency wave attenuate more rapidly than low frequency wave. Q is observed to be dependent on frequency. At higher frequency, in general, Q increases with frequency. In the Earth, Q is a function of depth, with the lowest Q values occurring in the upper mantle. In general, Q increases with seismic impedence, i.e. with increased material density and velocity.

The Q for P-waves in the Earth is systematically larger than Q for S-waves and thus refer to corresponding Q_p and Q_s respectively; $Q_p \simeq 9/4\ Q_s$. Table 2 gives approximate values of Q for different rocks.

Table 2

Q for different Rock types

Rock Type	Qp	Qs
Shale	30	10
Sandstone	58	30
Granite	250	70-150
Peridotite	1200	520
Outer Core	8000	0

The mechanisms of intrinsic attenuation are very sensitive to pressure and temperature. High heat flow area have more attenuation than colder regions. A schematic distribution of Q in a subduction zone is illustrated in Fig. 9.

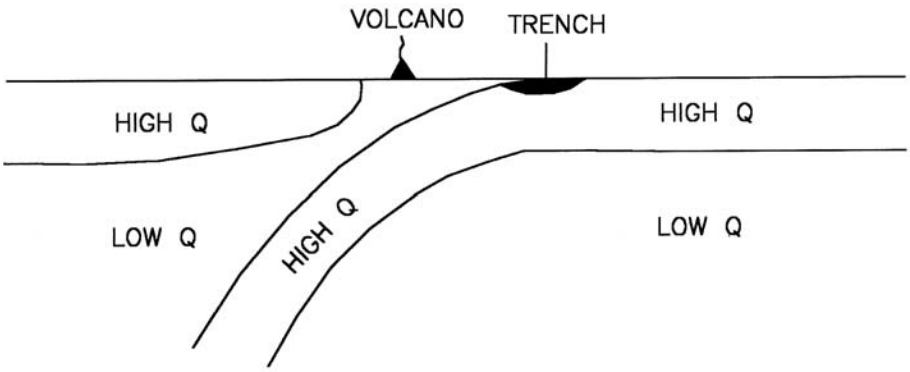

Fig. 9: Schematic distribution of Q in a subduction zone

In practice, it is difficult to separate intrinsic attenuation and scattering attenuation. Particularly, local earthquake records are strongly affected by scattering for local crustal heterogeneities, and scattering Q dominates. Scattering Q is usually determined from the decay of coda waves following S_g onsets, and is accordingly called Q_c. Unlike Q defined for intrinsic attenuation, Q_c is not a measure of energy loss per cycle, but rather, a measure of energy redistribution. Q_c is thus very much path dependent, and also strongly frequency dependent. A full discussion on this topic can be found in Aki and Richard (1980). An estimation of Q_c in Andaman Island region is discussed.

Seismic Diffraction

Seismic diffraction is defined as the transmission of energy by nongeometric ray paths. In optics, the classic example of diffraction is light "leaking" around the edge of an opaque screen. In seismology, diffraction occurs whenever the radius of curvature of a reflecting interface is less than the wavelengths of the propagating wave. Figure 10 shows the P wave & S wave rays that just graze the *core* and diffract into the *shadow zone*. The PKP waves are deflected downwards by the low velocities and observed at distances of 143^0 to 188^0. In fact, the edge of the boundary acts like a secondary source (Huygens' principle) and radiates energy forward in all directions.

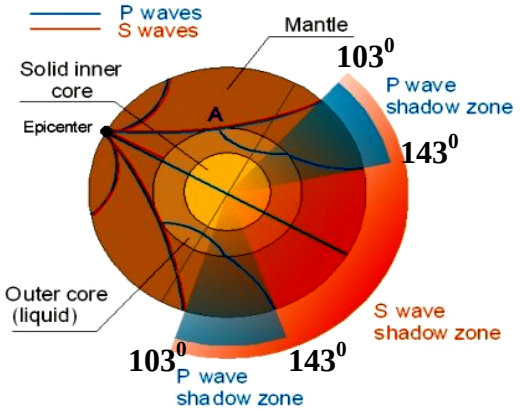

Fig 10 : Ray paths diffracted by the outer core.

The real Earth significantly deviate from simplified global one-dimensional models, thus scattering and diffraction affect not only amplitudes but also travel times. This has to be taken into account in recent development of automated travel-time measurement techniques.

EARTHQUAKE LOCATION

Manual Method

It is possible to get an approximate location of an earthquake without restoring to a computer. If the seismic network is dense and the earthquake is originated inside the network, the station with the earliest arrival can be approximated as the epicentre. This is called *earliest station method,* and it gives an estimate with a probable error of the same order as the station spacing.

Another approach is to contour the P-wave arrival times. This is an extension of the earliest station method. This may give fairly good estimate of the epicentre location if the network is dense enough. If the network is not dense, and consists of a few stations only, then the method is, however, not effective.

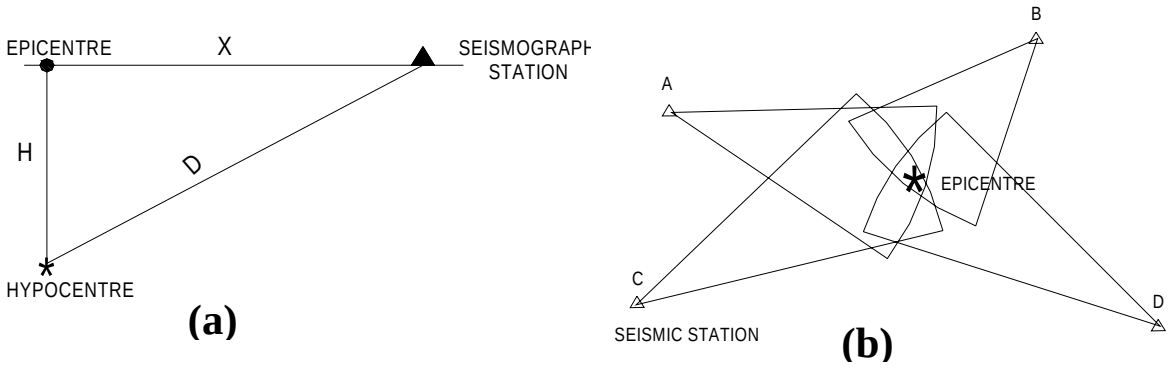

Fig.11: Manual location of earthquake epicentre.

A pretty good approximation of the epicentre can be made by *arc method or circle method* with three or more S-P times. Fig. 11a shows simple geometry of the epicentral distance X, hypocentral distance D and depth of focus (H) of an earthquake. If T_p is arrival time of the P wave and T_s is that of the S wave, then we can write:

$$T_p = \frac{D}{V_p} \quad \text{and} \quad T_S = \frac{D}{V_S}$$

where V_P and V_S are the velocity of the P-wave and S-wave respectively.

Thus we get

$$T_S - T_p = D\left(\frac{1}{V_S} - \frac{1}{V_p}\right) \tag{10}$$

Assuming $V_p/V_s = 1.73$, the hypocentre distance can be estimated as

$$D = 8\left(T_S - T_p\right) \tag{11}$$

where D is in kilometres, and S-P is in second.

After determining D at three or more stations, arcs can be drawn with each arc centred on the respective station and D equal to the arc length. As shown in the Fig. 11b, the epicentre lies in the region where the arcs overlap. This method is commonly used as a quick means of locating earthquakes. The *focal depth* (H) can be obtained as

$$H = (D^2\text{-}X^2)^{½} \tag{12}$$

Adding more observations will give additional intersections that theoretically should pass through the epicentre. In practice, error is always present, both in data and in assumptions, that the raypaths are straight and the Earth is homogeneous ; so scatter in the intersection usually occurs.

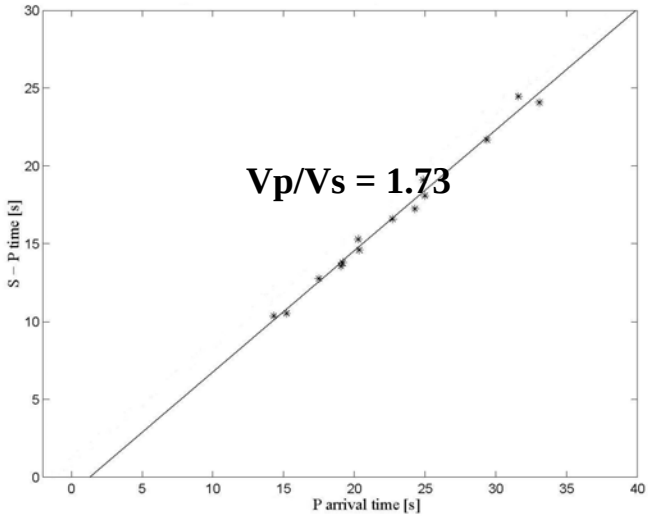

Fig 12 Wadati-plot showing origin time (13h 20m 1.2 s) and Vp/Vs.

The *origin time* of an earthquake can be determined with a very simple graphical technique, called *Wadati plot* (Wadati, 1933). The time separation of the P and S phase (t_s-t_p) is plotted against the arrival time of the P-wave. Since t_s-t_p = 0 at the hypocentre, a straight line fit on the Wadati diagram gives the origin time at the intercept with the P-arrival-time axis (Fig. 12).

Single-Station Location

In general, the arrival times of seismic phases at several stations are required to determine earthquake hypocentre and its origin time. It is, however, possible to use a single seismic station to obtain a crude estimate of earthquake location (Roberts et al., 1989). Single-station method requires three-component recordings of ground motion. Since P waves are vertically and radially polarized, the vector P-wave motion and the amplitude ratio AE/AN can be used to infer the back azimuth (against North) from station to the source.

If the vertical motion of the P-wave is upward, its radial component is directed away from the epicentre. If the vertical component of the P-wave is downward, the radial component is directed toward the epicentre. With suitable software, the ratio of the amplitude on the two horizontal components (AE/AN) can be used to find the vector projection of the P-wave along the azimuth to the seismic source. This has been implemented in the SEISAN software (Havaskov and Ottemoller, 2000).

Multi-station Location

When several stations are available, the earthquake location problem is resolved mathematically by *leas squares method* which gives a precise hypocentre location of the earthquake. The problem is to find the ‘ best’ origin-time (T_o) and the ‘best’ hypocentre (X_o, Y_o, Z_o). We assume some velocity model, usually a set of layers over a half space. Of course, given this assumption, the solution can only be used for local earthquakes, since at a distance of few hundred kilometres the sphericity of the Earth becomes a significant factor. Further, lateral heterogeneities in the velocity structure may become quite significant, and simple layered model will give inadequate results. However, we still use simple models to reduce computational complexities to locate the *local earthquakes*.

Geiger's (1912) method of least squares has been used by Lee and Lahr (1975) for developing the USGS *HYPO71* computer program. Let the

coordinates of the i^{th} station be (x_i, y_i, z_i), and the observed arrival time be τ_i. Let t_i be the computed arrival time based on a trial solution (i.e. an assumed origin time (t) and hypocentre (x,y,z). If the time residual

$$R_i = \tau_i - t_i \qquad (13)$$

is small, the Taylor expansion of it will give :

$$R_i = dt + \frac{\partial t_i}{\partial x} dx + \frac{\partial t_i}{\partial y} dy + \frac{\partial t_i}{\partial z} dz + e_i \qquad (14)$$

Since the travel time and derivatives can be computed from the given crustal model, we may obtain the adjustment vector (dt, dx, dy, dz) by least squares, i.e. demanding that the *error* e_i be such that :

$$\sum e_i^2 = \text{minimum} \qquad (15)$$

where $\sum$ denotes summation over all the stations, i.e. i = 1 to i = n.

COMPUTER PROGRAMS FOR EARTHQUAKE LOCATION

Given a set of arrival times, an earthquake location program is designed to find the origin-time and location of the earthquake, and to evaluate the limits of the error of the location. A secondary purpose of the program is to give feedback to the seismologist to aid in isolating and correcting reading errors. The program must be able to summarize, for a set of locations, the overall quality of the solutions and the average residuals for each station. Finally, the program must be able to compute the magnitude from either amplitude or coda duration measurements.

The hypocentre location produced by the program is the one which "best" matches the observed arrival times with the times computed by the given earthquake model. In this sense, the hypocentre location produced by the program is not the same as the true hypocentre if the velocity structure of the Earth model differs significantly form the true velocity structure of the Earth. The question arises, what is meant by the "best" solution? This is the solution that minimizes the *root mean square* (RMS) residual. That is, if we define R_i as the difference between the i^{th} observed and the i^{th} computed arrival time, and if we define RMS as:

$$RMS = \sqrt{\frac{\sum_{i=1}^{N} R_i^2}{N-1}} \qquad (16)$$

then the "best" solution is the one which minimizes RMS.

HYPO71 Program

There are many earthquake location programs. We first discuss the HYPO71 program of the USGS (Lee and Lahr, 1975), the one which is widely used and we are most familiar with. The basic input to HYPO71 are the *station list* (station coordinates), *velocity model*, *control parameters*, and of course the *arrival times*.

Station List

The station names used by HYPO71 may be up to 4 characters long e.g. SHIL (Shillong). P- delay (*station correction*) may be specified, and S- delay is calculated from the P- delay as

$$\text{S-delay} = \text{P-delay} \left(\frac{V_p}{V_s} \right) \qquad (17)$$

A positive residual would indicate that the observed time is larger than the computed time, and would be reduced by a positive delay.

P-wave Velocity Model

The computer program needs a reasonable velocity model to compute the travel-times. A plane layered P-wave velocity model based on available geological and geophysical information may be used for preliminary location of the earthquakes. The model then may be modified by trial and error method. The velocity model can be constrained from the observed arrival data of the recorded earthquakes. Time-distance plot of the direct P-arrivals (P_g and P*) may be used to estimate the velocity of the crustal layers, and P_n- arrivals may be used for the mantle-velocity estimate.

Velocity Ratio Vp/Vs

The computer program further needs a constant ratio of P to S-wave velocities (Vp/Vs) for computation of S-wave travel times. For preliminary location, an average value of Vp/Vs = 1.73 of the Earth's crust is used. However, Vp/Vs can be determined with a fair degree of accuracy by the *Wadati-plot* method (Wadati, 1933).

In *Wadati-plot* method, the S-P interval time is plotted against the P-arrival time (Fig. 12). The technique was originally suggested to estimate the origin time of an earthquake (Wadati, 1933), as discussed above, and later used

by many investigators for velocity-ratio estimates (e.g. Semenov, 1969; Utsu, 1969; Nersesov et al, 1971). If the wave paths from the hypocentre of an earthquake to an array of seismograph stations lie in a region of constant Vp/Vs, then the Wadati plot is linear and has a gradient Vp/Vs-1. This technique is useful because it yields a fairly accurate estimate of Vp/Vs without the knowledge of source parameters.

Control Parameters

Control over HYPO71 is achieved through the use of *reset list*. This is an optional series of upto 13 lines. Each line is used to reset one of 13 variables. If no reset list is present, HYPO71 will use a set of default values which are suitable for earthquakes recorded by the California network. The 13 variables on the reset list are as follows :

TEST (01) is the cut off value for RMS, below which Jeffreys' weighting of residuals is not used. It should be set to a value approximately equal to overall timing accuracy of P-arrivals in seconds. For small networks, less than 30 arrival times per earthquake, Jeffreys' weighting will not work well and should not be used.

TEST (02) limits simultaneous changes in epicentre and depth. If the epicentre adjustment is greater than this amount, the adjustment is recalculated with focal depth fixed. Test (02) should be set to a value approximately equal to station spacing in km.

TEST (03) is the critical F-value for the stepwise multiple regression (Draper and Smith 1966). It should be set according to the number and quality of P- and S- arrivals. If Test (03) is set to zero then simple multiple regression is performed. If Test (03) is set to 2 or greater then the iterative process may be terminated prematurely. A value between 0.5 and 2 is recommended.

TEST (04) is used to terminate the iterative location process. If the hypocentral adjustment is less than (04) the solution is terminated.

TEST (05) is used to control the maximum focal depth adjustment. If the adjustment (DZ) at any step is greater than Test (05) then DZ is reset to DZ/(K+1) where K = DZ/test(05). Test (05) should be set to a value approximately equal to half the range of focal depth expected.

TEST (06) : If no significant variable is found in the stepwise multiple regression, the critical value F is reduced to Test (03)/Test (06), and the

regression is repeated. If the Test (03) is set to less than 2, then Test (06) should be set to 1.

TEST (07), TEST (08) and TEST (09) are the coefficients used for calculating duration magnitude (Lee et al., 1972). According to the formula (using default values):

$$FMAG = -0.87 + 2\log T + 0.0035D \qquad (18)$$

where T = signal duration in second, and D = epicentral distance in km.

TEST (10) is used to control the maximum adjustment in latitude or longitude. If either adjustment exceeds Test(10) at some iteration, then a new reduced adjustment is calculated using Test(10).

TEST (11) is the maximum number of iterations in the solution process.

TEST (12) is used if the focal depth adjustment would put the hypocentre in the air. In that case, a new adjustment is calculated utilizing Test (12).

TEST (13) is used to control the radius of a sphere centered on the hypocentre location estimate. The RMS residual is calculated at ten points on the sphere to see if there is a nearby location with lower RMS than the final location.

HYPOELLIPSE Program

HYPOELLIPSE is modern version of HYPO71. Mainly the differences between this program and HYPO71 are discussed here. HYPOELLIPSE is complex and has a lot of options. Depending on the needs, this may or may not be an advantage. Compared to HYPO71, HYPOELLIPSE is not very stable. HYPO71 has not changed in the past 30 years, but HYPOELLIPSE probably changes every two or three months. HYPOELLIPSE has lots of options that are useful for research as well as for routine processing of data, but having many options makes the program more difficult to learn.

Instead of just one velocity model, HYPOELLIPSE allows up to ten velocity models to be specified. The V_P/V_S ratio may be varied in each layer. If detailed crustal velocity information is available, this flexibility is quite helpful. In addition to constant velocity layers over a half space one can also specify a linear increase over a half space. Also, in addition to calculating travel times using a model, up to three different travel-time models may be used. Elevation

corrections may be made based on station elevations, which is not done by HYPO71.

HYPOELLIPSE optionally compute the Vp/Vs ratio for each earthquake processed. The computed V_p/V_s ratio may be used in parts as a diagnostic tool. If the ratio is out of bounds, then a phase interpretation error is indicated. Spatial or temporal variations in V_p/V_S may also be studied.

In HYPOELLIPSE the *station list* contains a history of the station polarity, the station coordinates, the telemetry delay, and the gain as a function of time. Because of this, an arbitrarily long sequence of earthquakes may be proposed even if station parameters have changed during the sequence. As time progresses, the program automatically updates station parameters from the information in the station list. The station list allows independent P- and S-delays instead of having to use a fixed V_P/V_S ratio to compute S-delay, as in HYPO71.

Location error limits are specified by HYPOELLIPSE in terms of the error ellipsoid. This is the region in space in which there is 66% confidence that the earthquake occurred. The ellipsoid shape is determined entirely by the velocity model and the geometric relationship of the stations to the hypocentre. The scaling of the ellipsoid is based on an estimate of the probable reading errors of the arrival times. The error ellipsoid estimates the precision of the location but does not include any information on potential systematic error that might bias the location.

SEISAN Program

The SEISAN Program is now the most recent and becoming most popular seismic analysis system which provides a complete set of program for analysing earthquake data from analog as well as from digital records. The SEISAN system is built on collaborative efforts by the British Geological Survey, U.K. and by the University of Bergen, Norway (Havaskov and Ottemoller, 2000). With this system it is possible to enter phase readings manually, or pick them from digital records to locate events, plot epicentres etc. The program is very versatile; it can be used for local as well as for global events.

The routine processing normally produces magnitudes and hypocentres. Event statistics, depth section, b-value etc. can be plotted using this program. Fault-plane solution for individual event and composite solution for a group of events can be made by this program using first-motion data. Fault-plane solution from *wave form modeling* of the digital seismograms is an added

advantage with the program. In addition, *azimuth determination, spectral parameters*, *seismic moment*, *stress drop*, *seismic source radius* etc. can be determined by spectral analysis of the P- and S- waves for local earthquakes. Further, SEISAN contains some integrated research type programs like *coda Q, synthetic modeling,* 1-D *velocity inversion, joint hypocenter* location and a complete system for *site response* and *seismic hazard calculation.* In one word, SEISAN is the most versatile computer program now available for earthquake (analog + digital) data analysis. The program is made available on the website. www.ifif.uib.no/seismo/seisan.html. It has almost replaced the popular HYPO71 program.

LIMITATIONS OF PRECISION IN LOCATION

Depth and Origin Time

There is always certain amount of uncertainty in the observed arrival times and the Earth model used to compute the travel times. How these errors are mapped into spatial location errors depends on the geometric relationship of the stations to the hypocentre and on the phases that are used. Unless an earthquake is shallow and within a dense network, it is essential to have S-phase readings in addition to P-phase readings. The combination of P- and S-phases gives greater constraint on the origin time, and limits what could otherwise be an unbounded trade off between origin time and location.

Let us consider an earthquake at the centre of a circular array of stations (Fig. 13a). The P-phases will arrive simultaneously at all of the stations. This fixes the earthquake epicentre but places no constraint on depth. We can see why this is so by looking at a cross section of the problem. There is a trade-off between hypocentre depth and origin time. As shown in the figure 13a, for any depth, all the P- phases will arrive simultaneously. As depth is increased, the only effect is that the origin time must be earlier. Since there is no information about the origin time, there is no control over the depth. Just one S-phase reading would constrain the path length between the hypocentre and that station. This would serve to fix the origin time and hence the depth.

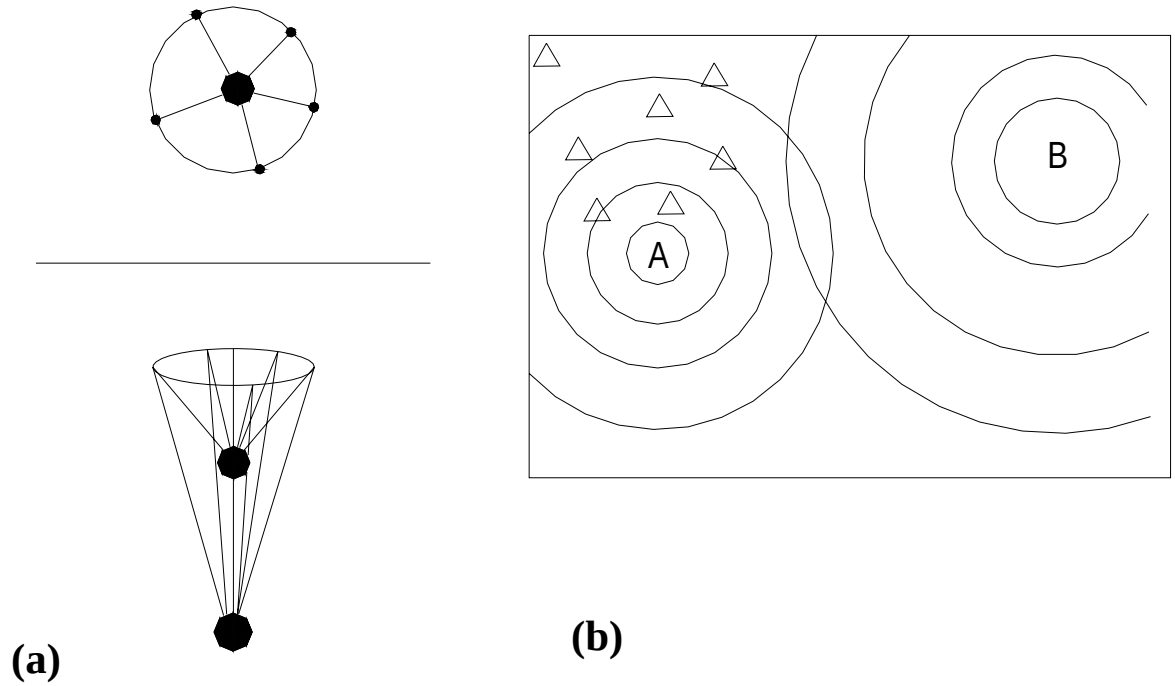

Fig 13: (a) Limitation in circular array and (b) limitation for the event outside the array.

If an earthquake occurs outside the network and only P-wave arrivals are available, the information that is used to get the distance to the epicenter is the curvature of the P-waves as they pass through the net. If the epicentre is very close to the net, as for the source at A in figure 13b, the curvature is significant. The source B, on the other hand, is further away and the curvature, as measured within the net, is less than that of the source A. If the source is farther away than about ten times the diameter of the net, then the curvature will be nearly plane as they pass through the net, and for all sources which are very far outside the net, the curvature is essentially the same. Therefore, as events get farther outside a network, S-phases become more important to constrain the distance to the source.

The depth of hypocentre inside a network may be difficult to constrain, even apart from those near the centre of a circular array. The problem is analogous to that of constraining the distance from the network to a distant earthquake. If the earthquake is shallow, relative to the station spacing, then the curvature is significant and the depth is well constrained. However, for deeper earthquakes it becomes progressively more difficult to constrain the hypocentre depth without S-wave readings. The conclusion is that minimum one or two reliable S-arrival data should be used to obtain a well constrained hypocentre solution.

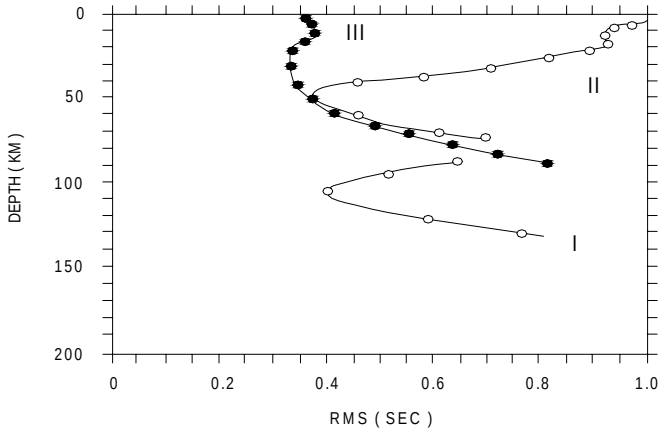

Fig 14: Plot illustrates the multiple minima problem

Multiple Minima Problem

Figure 14 illustrates a multiple minima problem. In the figure, the vertical axis is depth, increasing downward, and the horizontal axis is root mean square residual (RMS). The curve I shows a smooth decrease with depth to the minimum RMS and a smooth increase as depth increases past the minimum point. Not only is there just one minimum, but the minimum is very narrow. This is a well constrained solution.

The curve II presents more of a problem. There is a minimum at a depth of about 13 km followed by a small peak, and then another minimum at a depth of about 50 km. In this case, if the location program starts with a trial location near the surface, it will converge at the shallow minimum, even though the minimum at 50 km is actually the deepest or *global minimum*. The error bars for the shallow depth solution will indicate a well constrained minimum. The RMS will, however, indicate that there might be a problem with the solution. On the other hand, if the program started the solution at a depth below 20 km, the algorithm would converge at the global minimum of 50 km. The RMS returned would be much lower than for the shallow solution, but it is possible that the error bars would be wider if the slope near the global minimum is less than the slope near the shallow minimum.

The curve III has a minimum at the surface and another at a fairly shallow depth. The error bars returned for the 20 km depth solution will be rather large since the slope is so around that solution. One might note that the minimum near 20 km is less well constrained than the minimum at the surface, and choose the surface focus as the best solution. This is a mistake, the solution with the lowest RMS should be accepted.

Station Subset Problem

If we have a network with lots of stations and we locate a group of earthquakes, that group may often have a spatial distribution with a distinct trend. This can lead to believe that the distribution is due to some geological control such as a fault.

If the stations used in each location are reviewed it may be found that one or more of the stations was used for only a fraction of the earthquakes. It may be useful then to plot all the earthquakes for which a given station was used, and then plot all the earthquakes for which the station was not used. The two data sets may produce two distinct clusters which, when combined, give the trend seen in the complete data set. What we have then, is not a trend, rather an artifact; a more localized distribution whose computed location depends on the stations used. Various approaches for relocation of the earthquakes can be made to determine the true trend of seismicity.

EARTHQUAKE RELOCATION

To determine true trend of seismicity several techniques are applied to relocate the events. Principles of these techniques are briefly discussed.

Master Event Method

One approach in finding a true pattern in a set of earthquakes is called the *master event method*. We may start with one earthquake that is exceptionally well located and has readings for every possible phase at all the stations. It could be a main shock with very clear arrivals. Now, the *station delays* are so adjusted that the earthquake location has zero RMS. Then, another earthquake with nearly the same pattern of arrivals will locate near the master event, even if a different subset of stations is used.

Average Residual Method

Another approach is called the *average residual method*. Here we compute the average residual at each station for the entire set of earthquakes. Then use the averages as station delays and recompute the locations. The process can be iterated a few times. This will reduce the relative errors for this set of earthquakes.

Homogeneous Station Method

There could be scatter introduced into the solutions because of different combinations of stations being used in the solutions. An approach that is often useful in situations like this, is to find a subset of phase readings that were used for locating most of the events. Then those events may be relocated that have arrival times for all of these phase readings. All other events and phases may be excluded. This can be a very effective means of eliminating scatter, and may reveal a clear picture of the true hypocentral distribution. The method is also referred to as the *common phase method* (Lahr, 1996). In a small area, the epicentre locations are also independent of the velocity model error (Kayal, 1984, Kayal et al., 2003a).

Neither of the above methods, however, can improve the absolute error in source location for earthquakes in the group, but they reduce the relative location errors so that a pattern that would not have been apparent otherwise becomes clear.

Double-Difference (DD) Method

The double-difference (DD) technique, a theoretically based recent technique, also belongs to the relative earthquake location method (Got et al., 1994). This technique is based on the fact that if the hypocentral separation between two earthquakes is small enough compared to event-station distance, then the ray paths can be considered identical along their entire length. With this assumption, the differences in travel times for two earthquakes recorded at the same station may be attributed to the differences in spatial separation of the hypocenters. Thus the velocity-model errors are minimized without the use of station corrections.

The DD technique and the relocation algorithm (HYPO DD) are thoroughly discussed by Waldhauser and Ellsworth (2000) and Waldhauser (2001). Theoretical travel time differences are calculated based on the assumed 1D velocity model, and the residuals between the theoretical and observed times are minimized by an iterative procedure. When two events are close to each other compared to the event-station distance and to the scale of velocity heterogeneity in the broader hypocentral area, the residual between observed and calculated differential travel time for the two events is calculated as :

$$dr_k^{ij} = (t_k^i - t_k^j)^{obs} - (t_k^i - t_k^j)^{cal} \qquad (19)$$

where *t* is the travel time, superscripts *i* and *j* correspond to the two different events and the subscript *k* corresponds to a particular observation (i.e. one particular phase to one common station).

Joint Hypocentre Method

It is understood that for a given seismic station, the error in the predicted travel time is due to inaccuracies of the assumed velocity model. These deviations may occur anywhere along the travel paths, which may be divided into three categories : (i) deviations from the velocity structure near the source, (ii) deviations near the station, and (iii) deviations along the deeper travel path. For a single event-station pair, it is not possible to isolate the effects of these errors. On the other hand, if a *cluster* of earthquakes with approximately same location, occurs it is possible to determine a *station correction* that accounts for the inaccuracies of the model structure along the travel path and beneath the station (Fig.15). In this we include a correction term for each of the N stations and the residual or error at the i^{th} station for the j^{th} earthquake is given by :

$$\mathbf{r_{ij}} = \quad \mathbf{t_{ij} - (\tau_{ij} + S_i)} \qquad (20)$$

where t_{ij} is the observed arrival time, τ_{ij} is the computed travel time and S_i is the station correction term. In matrix form, it may be written as

$$\mathbf{r_j} = \mathbf{A_j}\ \mathbf{dx_j} + \mathbf{ds} \qquad (21)$$

where $\mathbf{r_j}$ is the Vector of residuals, $\mathbf{A_j}$ is matrix of Partial derivatives, $\mathbf{dx_j}$ is the Vector of origin time and hypocentre adjustment and **ds** is the Vector of station correction term. Solution of this system of equations is Joint Hypocentre Determination (JHD) and was proposed by Douglas (1967). Many authors (e.g. Herrmann et al., 1981 ; Pavlis and Booker, 1983 ; Pujol, 1988) proposed efficient inversion schemes for solving the Eq. 21 ; nearly all the schemes involve *singular value decomposition*.

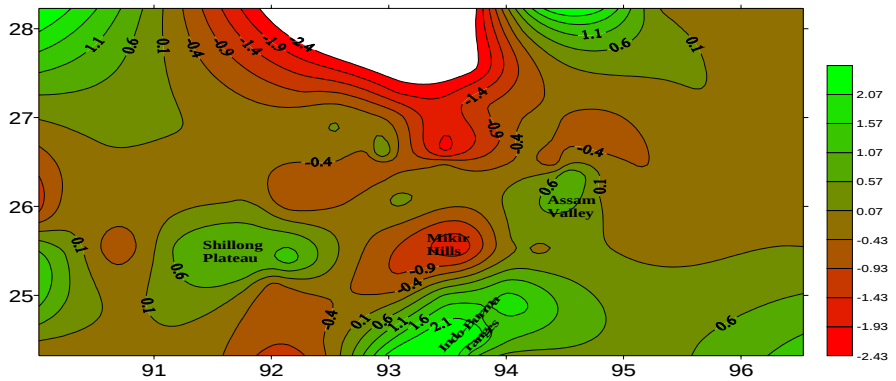

Fig 15: Station correction contours in NE India by the JHD (Bhattacharya et al., 2005)

SEISMIC TOMOGRAPHY AND RELOCATION

So far we have discussed about one dimensional plane layered velocity model for routine earthquake location. We, however, know that lateral heterogeneity exists at every depth in the Earth. For the last 50 years seismologists have been mapping gross velocity differences near the surface associated with variations between continental and oceanic crust and upper mantle. In the past 20 years, a concerted effort has emerged to map or image the three dimensional velocity structure inside the Earth using a method called *seismic tomography*.

'Tomo' is from a Greek word which means "slice". In tomography, we examine a series of two-dimensional slices from a three-dimensional object, and use the information to infer the internal structure of the three dimensional object. The beginning of tomography can be traced back to the discovery of x-rays by W. Roentgen in 1895.

Medical tomography and seismic tomography share some similarities, but they also have significant differences. In radiology, we measure the intensity of received x-rays, which is a function of the *absorption coefficient* of the travel path. In seismology, we measure a travel time which is a function of the *slowness* (i.e. inverse of velocity) along the ray path. In medical tomography, the x-ray path is a straight line. In seismology, the seismic- ray path is almost never a straight line. Also, in medical tomography, the source and detector locations are known exactly at all times. In seismic tomography, the source locations are unknowns which must be solved for, while inverting for the velocity structure. Figure 16 illustrates the basic differences in medical tomography and seismic tomography.

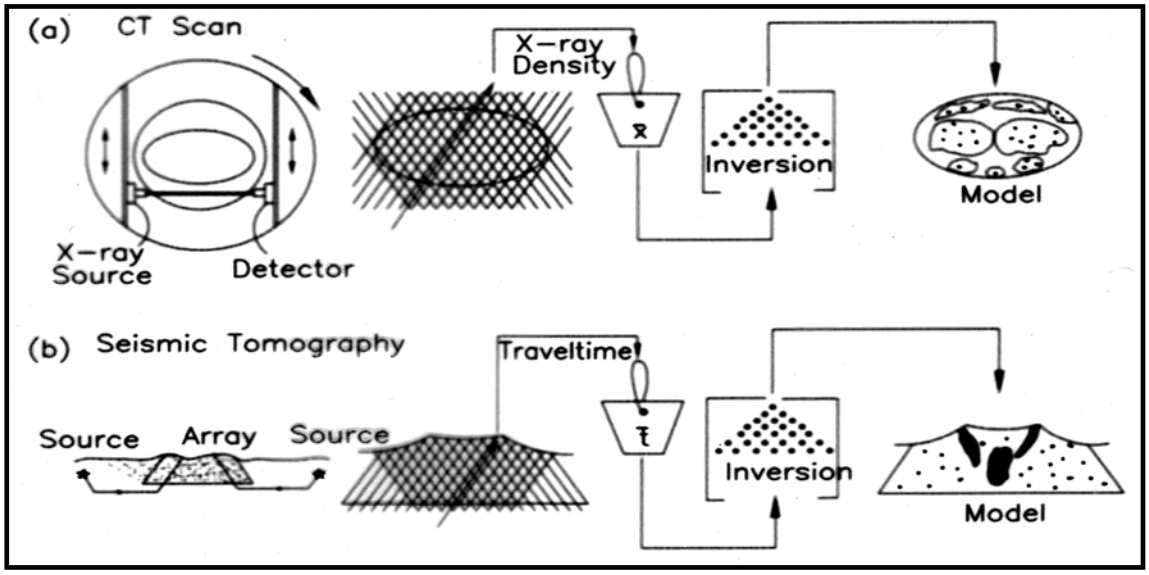

Fig 16. Schematic diagram showing differences in medical and seismic tomography.

During the early years of the development of seismic tomography, the technique was called *simultaneous inversion*. The idea was to get some information on the velocity structure of the Earth, and at the same time source parameters of the earthquakes were to be determined. In the mid-1970s, it occurred to a number of seismologists that since a seismic network may have hundreds of stations, and since only 4 stations are required to do a hypocentre inversion, all that extra information might be put to use to invert for the velocity structure of the Earth simultaneously with the hypocentre inversion. Crosson (1976 a,b) worked out the problem for the one-dimensional case, and Aki and Lee (1976) published the results of a three-dimensional inversion.

The principle in seismic tomography is discussed by Lay and Wallace (1995). A particular seismic phase with a travel time, T, is represented by a path integral through the medium as

$$T = \int_S \frac{ds}{v(s)} = \int_S u(s)ds \qquad (22)$$

where u (s) is the slowness [1/ v (s)] along the path. The *travel-time residual* relative to the reference Earth model may be caused by a velocity or slowness perturbation anywhere along the path. A change in velocity along the ray must perturb the raypath. The path integral through the medium perturbations should equal the observed travel-time residual :

$$\int_s \Delta u\,(s)\,ds = \Delta T = T_{obs} - T_{com}, \qquad (23)$$

where Δu (s) is the slowness perturbation to be determined.

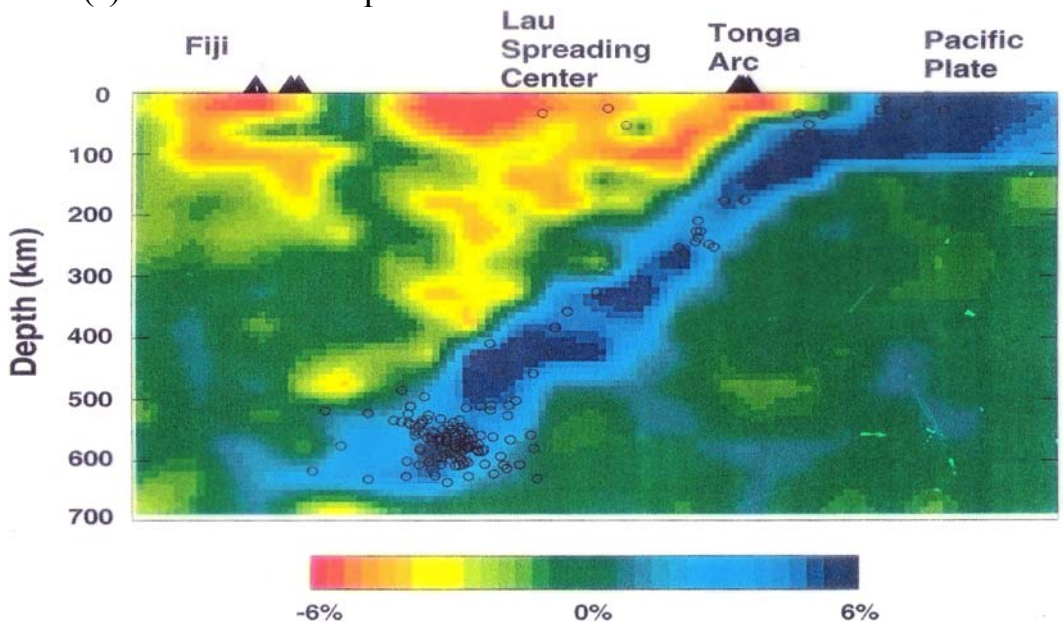

Fig 17. P-wave tomography in the Japan subduction zone (Zhao et al., 1992)

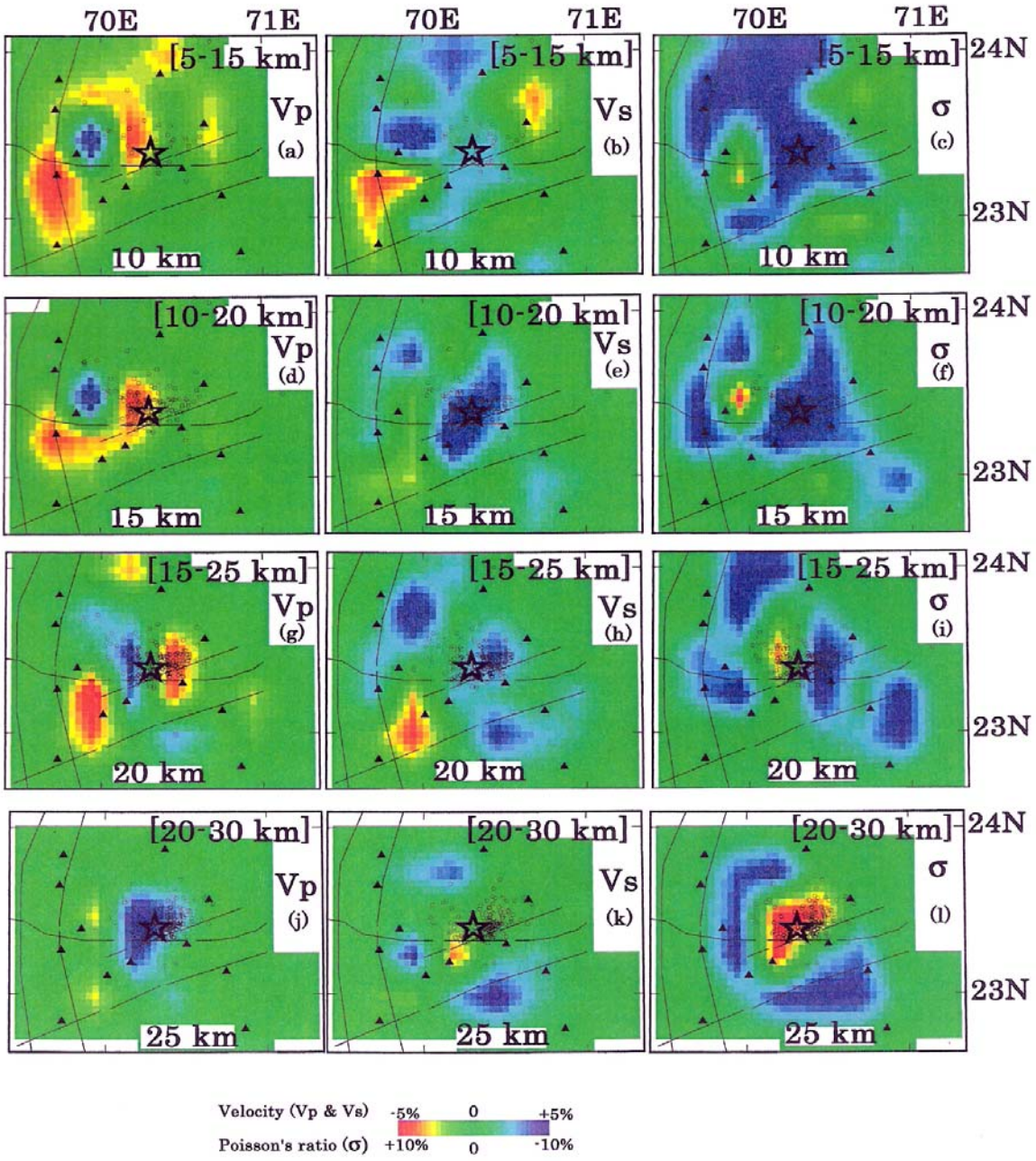

Fig.18: P, S and Vp/Vs tomography of the 2001 Bhuj earthquake Mw 7.7) source area, western India (Kayal et al, 2002)

Many authors have developed softwares for seismic tomography study (e.g. Aki and Lee, 1976; Thurber, 1981; Paige and Saunders, 1982 ; Um and Thurber, 1987). A state-of – the-art software is developed by Zhao et al. (1992). Although the conceptual approach of this software parallels that of Aki and Lee (1976), it has many additional features : (i) It is adaptable to a velocity structure that includes several complex shaped velocity discontinuities like the Moho discontinuity, dipping slab boundary etc., and images 3-D velocity variations in the model, (ii) It uses pseudo-bending technique of Um and Thurber (1987) and Snell's law to search the fastest ray. (iii) The LSQR

algorithm (Paige and Saunders, 1982) with damping regulation is used to solve the large and sparse system of observation equations, allowing a great number of data to be used to solve a large tomography problem. (iv) The nonlinear tomographic problem is solved by iteratively conducting linear inversions. In each iteration, perturbations to hypocentral parameters and velocity structure are determined simultaneously to determine the crustal and mantle structure in a region. The method has been used very successfully in Japan (Fig. 17) by Zhao et al. (1994 and 1996), in Alaska (Zhao et al., 1996), in Southern California (Zhao and Kanamori 1993, 1995), in northeast India (Kayal and Zhao, 1998), Bhuj 2001 earthquake source area (Kayal et al., 2002b), (Fig. 18), and in many subduction and volcanic zones (Zhao and Kayal, 2000; Mishra et al., 2005).

References :

Aki K., and Lee, W.H.K., 1976. Determination of three dimensional velocity anomalies under a seismic array using first P arrival times from local earthquakes, 1, A homogeneous initial model, *J. Geophys. Res*., 81: 4381-4399.

Aki, K. and Richards, P., 1980. *Methods of Quantitative Seismology*, Freeman, California.

Bullen, K. E., 1949. Compressibility-pressure hypothesis and Earth's interior. *Geophys. Supl*., 5: 355-368.

Bullen, K.E., 1965. *An Introduction to the theory of seismology*, (3rd ed.) Cambridge Univ. Press, London and New York.

Bullen, K.E. and Bolt, B.A., 1985. *An introduction to the theory of seismology,* 4th ed., Cambridge Univ. Press, U.K.

Cook, K. L., Algermissen, S.T. and Costain, J. L., 1962. The status of Ps converted waves in crustal studies. *J. Geophys. Res*., **67** :4769-4778.

Crosson, R.S. 1976 a. Crustal Structure modeling of earthquake data, Part-1: Simultaneous least squares estimation of hypocenter and velocity parameters. *J. Geophys. Res*., **81**: 3036-3046.

Crosson, R. S., 1976 b. Crustal structure modeling of earthquake data, Part 2: Velocity structures of the Puget Sound Region, Washington. *J. Geophys. Res*., **81** : 3036-3046.

Douglas, A., 1967. Joint Hypocentre Determination. *Nature*, **215**: 47-48.

Dresen, L. and Freystatter, S., 1976. Rayleigh channel waves for the inseam seismic detection of discontinuities. *J. Geophys. Res*., **42**: 111-129.

Evison, F.F., 1955. A coal seam as a guide for seismic energy. *Nature*, **176**: 1224-1225.

Ewing, M., Press, F. and Worzel, J. L., 1952. Further study of T phase, *Bull. Seism. Soc. Am*; **42** : 37-51.

Ewing, W.M., Jardetzky, W.S. and Press, F., 1957. *Elastic waves in layered media*, McGraw Hill, N.Y. pp. 380.

Field, E.H., and Jacob, K.H., 1995. A comparison and test of various site response estimation techniques, including three that are non reference-site dependent, *Bull.Seism.Soc.Am.,85*: 1127-1143.

Geiger, L., 1912. Probability method for the determination of Earthquake epicenters from the arrival time only, *Bull.St.Louis Univ*., **8**: 60-71.

Got, J. L., Fréchet, J. and Klein, F. W., 1994. Deep fault plane geometry inferred from multiplet relative relocation beneath the south flank of Kilauea, *J. Geophys. Res.,* **99**, 15,375-15,386.

Gutenberg, B., 1914. *Math Physics K1*. zu Gottingen

Gutenberg, B., 1944. Energy ratio of reflected and refracted seismic waves. *Bull.Seism. Soc. Am*., 34 : 85- 96.

Havaskov, J. and Ottemoller, L., 2000. *SEISAN: The earthquake analysis software,* Institute of Solid Earth Physics, Norway.

Herrin, E., 1968. Introduction to the 1968 Seismological Tables for P phases. *Bull. Seism. Soc. Am*., **58**: 1193-1201

Herrmann, R., Park, S. and Wang, C., 1981. The Denver earthquakes of 1967-1968, *Bull. Seism. Soc. Am*., **71** : 731-745.

Jeanloz, R., 1993, Chemical reactions at the Earth's core-mantle boundary: Summary of evidence and geomagnetic implications, in Relating Geophysical Structures and Processes, *The Jeffreys Volume (K. Aki and R. Dmowska, eds.), Am. Geophys. Union,* Washington, DC, 121-127.

Jeffreys, H. 1932. An alternative to rejection of observations, *Proc. Roy. Soc. A,* **137**: 78

Jeffreys, H., 1937. On the materials and density of the Earth;s crust. *Mon. Not. R.A.S., Geophys. Suppl*., **4,** 50.

Kayal, J.R., 1984. Microseismicity and tectonics at the Indian Pacific Plate Boundary : Southeast Wellington Province, New Zealand. *Geophys. J. R. Astr. Soc*. **77**: 567-592.

Kayal, J.R., 1986. Analysis of strong phases other than P and S from a microearthquake survey in the Wellington region, New Zealand. *Bull. Seism. Soc. Am.,* **76** : 1347-1354.

Kayal, J.R. and Zhao, Dapeng. 1998. Three dimensional seismic structure beneath Shillong Plateau and Assam Valley, northeast India, *Bull. Seism. Soc. Am.,* **88**: 667-676.

Kayal, J.R. Zhao, D., Mishra, O.P., De, Reena and Singh, O.P. 2002. The 2001 Bhuj Earthquake : Tomography evidence for fluids at hypocenter and its implications for rupture nucleation, *Geophys. Res. Lett*., **29** (24): 5.1-5.4.

Kennett, B.N.L. and Engdahl, E.R.,1991. Travel times for global earthquake location and phase identification, *Geophys. J. Int.,* 106,429-465.

Kennett B.L.N., Engdahl E.R. and Buland R., 1995. Constraints on seismic velocities in the Earth from travel times. *Geophys. J. Int.*, **122**, 108-124.

Krey, T. 1963. Channel waves as a tool of applied geophysics in Coal mining. *Geophysics*, **28**: 701-714.

Kulhanek, O. 1990. " Anatomy of Seismograms ", pp.178,Elsevier, Amsterdam, New York.

Lahr, J.C. 1992. Local earthquake location programs, In: Ed, W.H.K.Lee and D.H. Dodge, A course on PC based seismic networks, open file report (USGS), 92-441, pp 226-250.

Lay, T. 1989. Mantle, lower structure. In " The Encyclopedia of solid Earth Geophysics" (D.James, ed), pp 770-775. Van Nostrand-Rein hold, New York.

Lay, Thorne and Wallace, Terry, C. 1995. *Modern Global Seismology*, Academic Press, New York, USA, 521 p.

Lee, W.H.K., Bennett, R.E. and Meagher, K.L.,1972. A method of estimating magnitude of local earthquakes from signal duration, *open file report, U.S. Geol. Surv.*

Lee, W.H.K. and Lahr, J.C. 1975. Hypo-71 : A computer program for determining hypocenter, magnitude and first motion pattern of local earthquakes. *Open file report, U.S. Geol. Surv.* Rev. Ed.

Lehmann, I. ,1935. P^1. *Pub. Bur. Cent. Seism. Internat*, A. 14, 3.

Love, A.E.H., 1911. *Some problems of geodynamics*, Cambridge Univ. Press, London.

Mishra, D.C., Chandrasekhar, D.V. and Singh, B., 2005. Tectonics and crustal structures related to Bhuj earthquake of January 26, 2001 : based on gravity and magnetic surveys constrained from seismic and seismological studies, *Tectonophysics*, **396** : 195-207.

Nersesov, I.O., Semenov, A.N. and Simbireva, I.G., 1971. Space-time distribution of ratios of travel times of P and S waves in the Garm Region. *Experimental Sesimology*, pp. 334-345, Science Publishers. Moscow.

Oldham, R.D. 1906. Constitution of the interior of the Earth as revealed by earthquakes. *Q. J. Geol. Soc*. 62, 456-475.

Paige, C. C. and Saunders, M. A., 1982. LSQR: sparse linear equations and least squares problems, *ACM Transactions on Mathematical Softwares,* **8(2)**: 195-2009.

Pavlis, G. and Booker, J. ,1983. Progressive multiple event location (PMEL). *Bull. Seism. Soc. Am*., **73**: 1753-1777.

Pujol, J., 1988. Comments on the joint determination of hypocenters and station corrections. *Bull. Seism. Soc. Am*., **78**: 1179-1189.

Rayleigh, Lord 1885. On waves propagated along the plane surface of an elastic solid. *Proc. Lond. Math. Soc*., 17, 4.

Roberts, R.G., Christoffersson, A. and Cassidy, F. 1989. Real time event detection, phase identification and source location estimation using simple station three component seismic data, *Geophys. J. Roy. Astro. Soc*., **97** : 471-480.

Semenov, A.N. 1969. Variations in travel time of transverse and longitudinal waves before violent earthquakes. *Bull. Acad. Sci. USSR*, *Phys. Solid Earth (English Trans*.) **3** : 245-248.

Thurber, C.H. 1981. Earth structure and earthquake locations in the Coyote Lake area, Central California. *Ph.D. thesis*, Massachusetts Institute of Technology, USA.

Um, J. and Thurber, C. ,1987. A fast algorithm for two-point seismic ray tracing. *Bull. Seism. Soc. Am*., **77** : 972-986.

Utsu, T., 1969. Aftershocks and earthquake statistics, 1. Some parameters which characterise an aftershock sequence and their interrelations. *J. Fac. Sci*. , *Hokkaido Univ., Geophys.* 3 : 129-195.

Wadati, K. 1933. On the travel time of earthquake waves, Part II, *Geophys. Mag.*, **7** : 101-111.

Waldhauser, F. and Ellsworth, W., 2000. A double difference earthquake location algorithm: method and application to the northern Hayward Fault, California, *Bull. Seism. Soc. Am.*, **90**: 1353-1368.

Waldhauser, F., 2001. HypoDD: A computer program to compute double-difference earthquake locations, *U.S. Geol. Surv. open-file report* , 01-113, Menlo Park, California,

Wiechert, E. and Zoppritz, K., 1907. *Math Phys. Kl.,* zu Gottingen, 529.

Zhao, D., Hasegawa, A. and Horiuchi, S., 1992. Tomographic Imaging of P and S wave velocity structure Beneath Northeast Japan. *J. Geophys. Res*., **97** : 19,909-19,928.

Zhao, D., A. Hasegawa, H. Kanamori (1994) Deep structure of Japan subduction zone as derived from local, regional, and teleseismic events. J. Geophys. Res. 99, 22313-22329

Zhao , D. Kanamori, H. and Humphreys, E. 1996. Simultaneous inversion of local and teleseismic data for the cruist and mantle structure of southern California. *Phys. Earth Planet. Inter.,* **93**, 191-214.

Zhao, D. and Kanamori, H. 1993. The 1992 Landers earthquake sequence: earthquake occurrence and structural heterogeneities. *Geophys. Res. Lett*., **20**, 1083-1086.

Zhao, D. and Kanamori, H., 1995. The 1994 Northridge earthquake: 3-D crustal structure in the rupture zone and its relation to the aftershock locations and mechanisms. *Geophys. Res. Lett*., **22**, 763-766.

Zhao, D.and Kayal, J.R. (2000) Impact of seismic tomography on Earth sciences. *Current Science,* **79**, 1208-1214.